

# Correction Scheme for Multiple Correlated Statistical Tests in Local Shape Analysis

Martin Styner<sup>1</sup> and Guido Gerig<sup>2</sup>

<sup>1</sup> M.E. Müller Research Center for Orthopaedic Surgery, Institute for Surgical Technology and Biomechanics, University of Bern, P.O. Box 8354, 3001 Bern  
`martin.styner@ieee.org`

<sup>2</sup> Department of Computer Science, University of North Carolina at Chapel Hill, CB#3175, Sitterson Hall, Chapel Hill, NC 27599-3175

**Abstract.** In neuroimaging research shape analysis has become a field of great interest due to the ability to locate morphological brain changes between different groups. Currently, most local shape analysis approaches fail to correct for their high number of correlated statistical tests. This results in an overly optimistic estimate of the local shape analysis. This paper presents a correction scheme for objects described by a parametrized 3D closed surface description. The scheme decomposes the object surface into overlapping planar images via a cylindrical equal area projection of the parameterization. The images are individually analyzed with the SnPM/SPM package using a voxel-level non-parametric multiple testing procedure based on permutation tests. The correction scheme employs conservative tests resulting in a pessimistic estimate. We present an application of the correction scheme in the analysis of the shape similarity of lateral ventricles.

## 1 Introduction

Quantitative morphologic assessments of individual brain structures most often entail segmentation followed by volume measurements. Volume changes are intuitive features as they may explain atrophy or dilation of structures due to illness. On the other hand, structural changes at specific locations are not sufficiently reflected in global volume measurements. In order to capture such changes, researchers have developed in recent years new methods for shape description and analysis. In their current framework, most methods perform large sets of 1000 or more uncorrected, correlated statistical tests. This often leads to either incorrect or highly optimistic local statistics. This paper presents a conservative correction scheme that can be applied to parametrized shape descriptions.

One of the first to mathematically analyze shape changes was D'Arcy Thomson [1] in his ground-breaking book *On Growth and Form*. Most shape analysis methods are strongly influenced by D'Arcy's work.

Several researchers proposed shape analysis via deformable registration to a template [2–4]. Inter-subject comparisons are made by analyzing and comparing the individual deformable transformations. This analysis of the transformation

fields has to cope with the high dimensionality of the transformation, the template selection problem and the sensitivity to the initial position. Several studies have shown stable shape analysis results, but the computation of correct statistical significance values has as of yet only been addressed by a few [5, 6].

Bookstein et al. [7] and Dryden et al. [8] presented some of the first mathematical methods for 3D shape analysis based on object specific sampled descriptions. The shape analysis of densely sampled 3D Point Distribution Models (PDM) and their deformations was first investigated by Cootes and Taylor [9]. Motivated by their experiments, Gerig et al. [10] proposed a shape analysis based on a parametric boundary description called SPHARM [11] (described in section 2.1). The SPHARM shape analysis approach was extended by Styner et al. to use the implied PDM [12], a method recently also used by Shen et al. [13]. Pizer et al. [14, 15] proposed shape analysis methods for a 3D medial shape description called M-rep. They proposed a fixed topology sampled medial model with implicit correspondence that is fitted to individual objects.

The issue of correcting for multiple correlated statistical tests in the local shape analysis has not been addressed by any PDM, SPHARM or medial shape analysis method. It has been addressed though in the field of functional neuroimaging using a voxel-by-voxel statistical analysis to find group differences. Friston et al. [16] and Holmes et al. [17] developed techniques for these correlated voxel-by-voxel tests and embedded them into the open-source projects Statistical Parametric Maps (SPM) and Statistical non-Parametric Maps (SnPM).

This paper presents a novel, conservative correction scheme based on the SnPM package applied to the SPHARM shape analysis. It can also be applied to other closed parametrized shape descriptions. In the next sections, we discuss our methods, followed by results of a shape analysis study of lateral ventricles.

## 2 Methods

This section first describes the SPHARM shape description, followed by its group difference shape analysis that is uncorrected for multiple correlated statistical tests. The following subsection then describes SnPM’s correction scheme for multiple tests. For the processing in SnPM we compute a decomposition of the 3D surface into planar images as described in the last subsection.

### 2.1 SPHARM shape description

The SPHARM description is a parametric surface description that can only represent objects of spherical topology [11]. The spherical parameterization is computed via optimizing an equal area mapping of the 3D voxel mesh onto the sphere and minimizing angular distortions. The basis functions of the parameterized surface are spherical harmonics. Based on a uniform icosahedron-subdivision of the spherical parameterization, we can obtain a Point Distribution Model (PDM) directly from the coefficients via linear mapping[18]. Correspondence of SPHARM is determined by normalizing the parameterization to the first order ellipsoid[12].

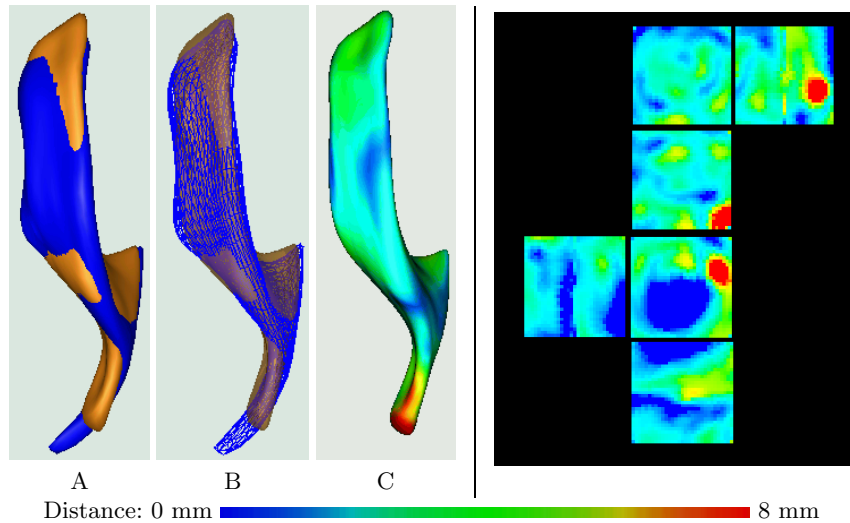


**Fig. 1.** Left: visualization of the distance map between the right lateral ventricles of a twin-pair (superior view). A: the two ventricles after alignment and scaling. B: Same as A, one ventricle shown transparent and the other as grid-mesh. C: distance map with color-coded distance at each boundary-point. Right: The same distance map after decomposition into 6 planar images for testing in SnPM. The images are arranged as if unrolled from the unit sphere. A considerable overlap (min. 25% on each side) between the images is visible, as well as large distortions towards the image edges.

## 2.2 SPHARM shape analysis

In this subsection, we briefly discuss the SPHARM shape analysis previously detailed in [12] and [15]. Alignment and scaling of the objects are two important issues in shape analysis that are not discussed in detail here. In the presented study, the objects were rigidly aligned using a rigid-body Procrustes-alignment [19] and uniformly scaled to the same volume.

**Feature maps** - For each SPHARM object, we compute a feature map, which is composed of a single distance value per point on the PDM surface. This distance map represents the local (signed or unsigned) Euclidean distances either to a template object or to a designated comparison object, e.g. in similarity studies (Fig. 1).

**Statistical maps** - We perform two different types of statistical analysis in order to test for group differences: a global and a local shape analysis. The global shape analysis is based on one scalar global value for each analyzed object. The global values commonly used are the average, the median, or quantile values. The global analysis entails only a single or a few statistical tests and thus a correction for multiple tests is not needed. This becomes necessary in the local analysis, since a statistical test is computed for every location on the object,

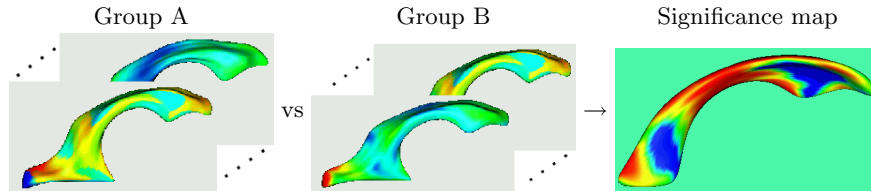


**Fig. 2.** Schematic visualization of the statistical map computation: For two groups of objects, every corresponding location is compared in a statistical test yielding a statistical map. The visualization of the groups shows the color-coded feature values. The significance map shows the color-coded significance.

which results in thousands of correlated standard group mean difference tests yielding a statistical significance map (see Fig. 2).

### 2.3 Statistical analysis via the SPM/SnPM package

We propose to perform the correction for multiple testing using the non-parametric permutation approach in the SnPM package [17], which is part of the SPM package [16]. This package was built for the voxel-level analysis of 3D volumetric neuroimaging experiments mostly in functional MRI, PET and SPECT. Since our data is 3D surface data and not volumetric data, we have developed a scheme that decomposes the surface into planar images as described in the next section.

The SnPM permutation approach accounts for the multiple testing problem using a locally pooled smoothed variance estimate [20]. In this procedure, the permutation tests are performed first over all possible group-relabelings of the subjects, and then over all voxels from a volume of interest. The resulting variance estimates for the maximal voxel statistic are smoothed using a 2D kernel. The size of the kernel and the size of the volume of interest for the permutations is the same. This testing procedure has *strong* control over experiment-wise Type I errors (falsely declaring a region to be significant) and can be regarded as a conservative test [17].

### 2.4 Planar decomposition of spherical parameterization

This section describes the decomposition of the 3D surface data into a set of planar images. These images are individually processed as single slice data with the SnPM package. In summary, the decomposition is based on the Lambert azimuthal projection, a cylindrical equal area projection, of an image grid onto the spherical parameterization of the 3D surface. The center of the image grid is chosen at 6 different locations resulting in 6 planar images (Figure 1). The decomposition scheme is schematically visualized for a single image in Figure 3. It is noteworthy that the 3D object surface parameterization and the cylindrical projection are both area-preserving.

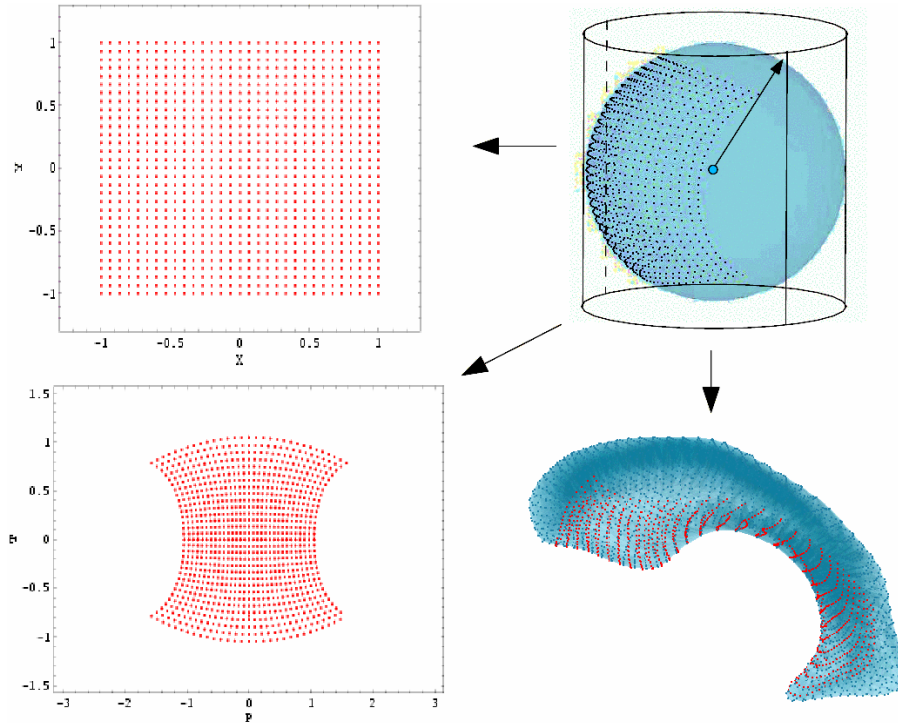


**Fig. 3.** Planar decomposition of a spherically  $(\phi, \theta)$  parametrized 3D surface using a cylindrical equal area projection. Top left: the unrolled cylindrical image grid. Top right: the cylindrical grid projected unto the unit sphere. Bottom left: the projected grid visualized in spherical coordinate space  $(\phi, \theta)$ . Bottom right: The 3D surface points corresponding to the projected grid determined by the  $(\phi, \theta)$  parameterization.

As the first step of the decomposition scheme, an image grid is defined on a cylinder, which is projected onto the sphere. The sampling of the image grid is chosen to be of the same order as the sampling of the 3D surface ( $64 \times 64$  pixels per image). Then, the spherical  $(\phi, \theta)$  coordinates are determined for the projected grid. The feature value for each grid node is now computed via the parameterization of the 3D surface.

This procedure is performed separately at 6 different locations on the sphere for the center of the image grid:  $(0,0)$ ,  $(\pi/2,0)$ ,  $(\pi,0)$ ,  $(3\pi/2,0)$ ,  $(0,\pi/2)$ ,  $(0,-\pi/2)$ . At the equator latitude, the overlap between each two images is 25%, resulting in a minimal total overlap of 75%. This overlap between the images is necessary to minimize the influence of the distortions introduced by the projection.

After computation of the statistical significance for each image separately in SnPM, the 6 images are re-assembled on the 3D object surface. In overlapping image regions, the significance values are averaged.

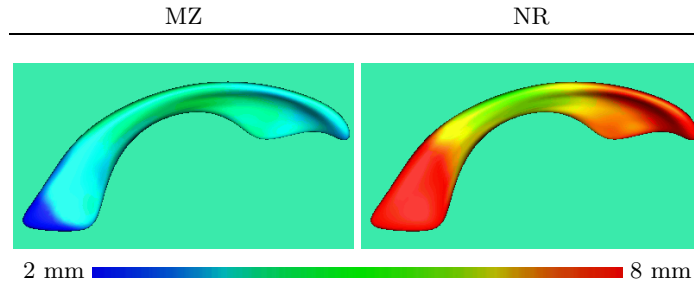


**Fig. 4.** Average distance maps visualize the pointwise averaged local distances for the Monozygotic twin group (MZ) and the non-related subject group (NR). These are shown color-coded according to the provided colormap on the average structure.

### 3 Results

This section describes the proposed correction scheme applied to a shape similarity study of the right lateral ventricle, a fluid-filled space in the human brain. The segmentation was performed with a single gradient-echo MRI automatic brain tissue classification [21]. Postprocessing with 3D connectivity, morphological closing and minor editing provided simply connected 3D objects.

There are 2 groups of subjects each consisting of 20 subjects: a Monozygotic (MZ) twin group and a non-related subject group (NR). We compared the similarity of the right lateral ventricle between two monozygotic twins, and between two non-related subjects. The groups are age and gender matched. Due to the large age range and the presence of both genders, the analysis was done after correction for gender and age influence (linear least square model).

The average surface distance between two surfaces was used as a global shape measure of similarity. This measure was highly significant between the two groups ( $p = 0.0006$ ). The local surface distance was used as a local shape measure (see Fig. 1). The local distance maps were pointwise averaged for every subject group resulting in two average distance maps (see Fig. 4). These maps show that the MZ group has considerable smaller average distance values than the NR group across the whole object except for the central part.

In the uncorrected statistical analysis a standard mean difference test is applied for every surface point. The result of this analysis is visualized in Figure 5 (left). The analysis shows significant local shape differences between the groups across the whole object with exception to a small central area. This analysis is most likely too optimistic, since the correlation between the local statistical tests has not been taken into account. The local statistical analysis, corrected according to the presented scheme, is visualized in Figure 5 (right). Clearly, a loss of significance is visible. Since the presented testing scheme is a conservative test for Type I errors, the regions of significant local shape differences are correct, but the analysis seems to be too pessimistic regarding non-significant regions.

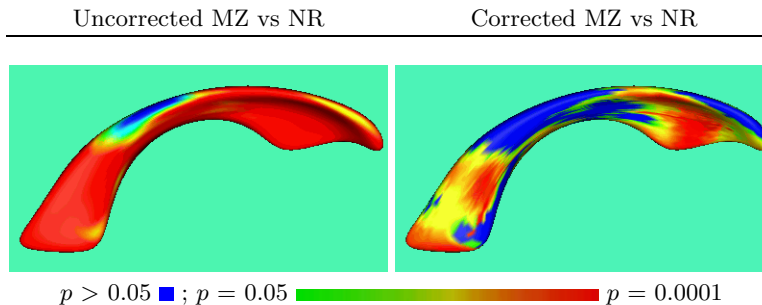


**Fig. 5.** Statistical maps visualize the locations of significant difference between groups. The distances are color-coded according to the provided colormap. Left: uncorrected analysis. Right: corrected analysis. A loss of significance is clearly visible.

## 4 Conclusions

We have presented a novel correction scheme for local shape analysis with multiple correlated statistical tests. The scheme decomposes the object-surface into planar images, which are analyzed with the SnPM package. The correction scheme employs conservative tests, resulting in a pessimistic estimate. The scheme has been applied to objects described with the SPHARM shape description, but can be applied to other parametrized, closed shape descriptions.

As a follow-up to this study, researchers at the UNC laboratory are developing a correction scheme directly operating in the 3D object space.

## 5 Acknowledgments

We are thankful to Christian Brechbühler for providing the software for SPHARM surface parameterization and description. Douglas Jones and Daniel Weinberger at NIMH, Clinical Brain Disorder Branch (Bethesda, MD), kindly provided the original MRI datasets of the ventricle data. Jeffrey Lieberman and the neuro-image analysis lab at UNC Chapel Hill, Department of Psychiatry, provided the segmentations of the ventricle data. Maya Styner is acknowledged for editorial assistance.

## References

1. D. Thomson, *On Growth and Form*, Cambridge University Press, second edition, 1942.
2. C. Davatzikos, M. Vaillant, S. Resnick, J.L. Prince, S. Letovsky, and R.N. Bryan, “A computerized method for morphological analysis of the corpus callosum,” *Journal of Computer Assisted Tomography*, vol. 20, pp. 88–97, Jan./Feb 1996.
3. S. Joshi, M. Miller, and U. Grenander, “On the geometry and shape of brain sub-manifolds,” *Pat. Rec. Art. Intel.*, vol. 11, pp. 1317–1343, 1997.

4. J.G. Csernansky, S. Joshi, L.E. Wang, J. Haller, M. Gado, J.P. Miller, U. Grenander, and M.I. Miller, "Hippocampal morphometry in schizophrenia via high dimensional brain mapping," *Proc. Natl. Acad. Sci. USA*, vol. 95, pp. 11406–11411, September 1998.
5. P. Thompson, J. Giedd, R. Woods, D. MacDonald, A. Evans, and A. Toga, "Growth patterns in the developing brain detected by using continuum mechanical tensor maps," *Nature*, vol. 404, pp. 190–193, 2000.
6. J. Cao and K.J. Worsley, "The detection of local shape changes via the hotteling's  $T^2$  fields," *Annals of Statistics*, vol. 27, pp. 925–942, 1999.
7. F.L. Bookstein, "Shape and the Information in Medical Images: A Decade of the Morphometric Synthesis," *Comp. Vision and Image Under.*, vol. 66, no. 2, pp. 97–118, May 1997.
8. I.L. Dryden and K.V. Mardia, "Multivariate shape analysis," *Sankhya*, vol. 55, pp. 460–480, 1993.
9. T. Cootes, C.J. Taylor, D.H. Cooper, and J. Graham, "Active shape models - their training and application," *Computer Vision and Image Understanding*, vol. 61, pp. 38–59, 1995.
10. G. Gerig, M. Styner, M.E. Shenton, and J.A. Lieberman, "Shape versus size: Improved understanding of the morphology of brain structures," in *Medical Image Computing and Computer-Assisted Intervention*, 2001, pp. 24–32.
11. C. Brechbühler, G. Gerig, and O. Kübler, "Parametrization of closed surfaces for 3-D shape description," *Computer Vision, Graphics, Image Processing: Image Understanding*, vol. 61, pp. 154–170, 1995.
12. G. Gerig, M. Styner, D. Jones, D. Weinberger, and J. Lieberman, "Shape analysis of brain ventricles using spharm," in *Mathematical Methods in Biomedical Image Analysis*. 2001, pp. 171–178, IEEE press.
13. L. Shen, J. Ford, F. Makedon, and A. Saykin, "Hippocampal shape analysis surface-based representation and classification," in *SPIE-Medical Imaging*, 2003.
14. S. Pizer, D. Fritsch, P. Yushkevich, V. Johnson, and E. Chaney, "Segmentation, registration, and measurement of shape variation via image object shape," *IEEE Transactions on Medical Imaging*, vol. 18, pp. 851–865, Oct. 1999.
15. M. Styner, G. Gerig, J. Lieberman, D. Jones, and D. Weinberger, "Statistical shape analysis of neuroanatomical structures based on medial models," *Medical Image Analysis*, 2003, to appear.
16. KJ Friston, AP Holmes, KJ Worsley, JP Poline, CD Frith, and RSJ Frackowiak, "Statistical parametric maps in functional imaging: A general linear approach," *Human Brain Mapping*, , no. 2, pp. 189–210, 1995.
17. T.E. Nichols and A.P. Holmes, "Nonparametric analysis of pet functional neuroimaging experiments: A primer with examples," *Hum Brain Mapp*, vol. 1, no. 15, pp. 1–25, Jan 2001.
18. A. Kelemen, G. Székely, and G. Gerig, "Elastic model-based segmentation of 3d neuroradiological data sets," *IEEE Transactions on Medical Imaging*, vol. 18, pp. 828–839, October 1999.
19. F.L. Bookstein, *Morphometric Tools for Landmark Data: Geometry and Biology*, Cambridge University Press, 1991.
20. AP Holmes, RC Blair, JDG Watson, and I Ford, "Nonparametric analysis of statistic images from funtional mapping experiments," *J Cereb Blood Flow Metab*, vol. 1, no. 16, pp. 7–22, 1996.
21. K. Van Leemput, F. Maes, D. Vandermeulen, and P. Suetens, "Automated model-based tissue classication of mr images of the brain," *IEEE Transactions on Medical Imaging*, vol. 18, no. 10, pp. 897–908, 1999.